Humus forms and metal pollution in soil

Servane Gillet, Jean-François Ponge

Humus forms and metal pollution in soil

S. GILLET & J.F. PONGE

Museum National d'Histoire Naturelle, Laboratoire d'Écologie Générale, 4 avenue du Petit-Chateau, 91800 Brunoy, France

Short title: *Humus forms and metal pollution*

Summary

Smelters in northern France are a serious source of soil pollution by heavy metals. We have studied a poplar plantation downwind of an active zinc smelter. Three humus profiles were sampled at increasing distance from the smelter, and the thickness of topsoil horizons was measured along a transect. We analysed the vertical distribution of humus components and plant debris to assess the impact of heavy metal pollution on the humus forms and on soil faunal activity. We compared horizons within a profile, humus profiles between them, and traced the recent history of the site.

Near the smelter, poplar trees are stunted or dead and the humus form is a mor, with a well-developed holorganic OM horizon. Here faunal activity is inhibited, so there is little faecal deposition and humification of plant litter. At the distant site poplar grows well and faunal activity is intense, so there are skeletonized leaves and many organo-mineral earthworm and millipede faecal pellets. The humus form is a mull, with a well-developed hemorganic A horizon. The passage from mor to mull along the transect was abrupt, mor

Correspondence: J.F. PONGE. E-mail: jean-francois.ponge@wanadoo.fr

Received 13 December 2001; revised version accepted 23 March 2002

turning to mull at 250 m from the smelter, though there was a progressive decrease in heavy metal deposition. This indicates that there was a threshold (estimated to 20 000 mg $Zn.kg^{-1}$) in the resilience of the soil foodweb.

Introduction

Today, in northern France, numerous sites are polluted by heavy metals (Balabane *et al.*, 1999; Sterckeman *et al.*, 2000). In the Nord-Pas-de-Calais district alone, more than 125 sites polluted by smelting have been registered (Recensement 1996 des Sites et Sols Pollués, Ministère de l'Aménagement du Territoire et de l'Environnement). There are two sources of pollution: (a) the atmospheric emission of metals from smelters, and (b) dumping of slag rich in heavy metals. Soil surface horizons suffer most from atmospheric fallout (James & Riha, 1986). Thus, when their buffering capacity is exceeded, they become biologically less diverse (Belotti & Babel, 1993). They also exhibit severe physical (structure, texture) and chemical (ion leaching) changes (Schvartz *et al.*, 1999; Sterckeman *et al.*, 2000).

Direct and indirect effects of heavy metal pollution on the soil fauna have been observed and demonstrated experimentally (Bengtsson *et al.*, 1983; Hågvar & Abrahamsen 1990; Grelle *et al.*, 2000). Such impacts have far-reaching consequences on the processes of humification and mineralization and on the development of humus forms (Ponge, 1999). In particular, a reduction in faunal activity may result in the accumulation of undecayed plant debris on the ground surface, due to the absence of litter comminution and faecal deposition (Ponge *et al.*, 2000). Soil microbial communities are also severely affected by heavy metal pollution, which results in a decrease in the decomposition rate of organic matter (Balabane *et al.*, 1999) and avoidance of litter by soil animals (Tranvik & Eijsackers, 1989).

We aimed in this study to assess the impact of heavy metal pollution on humus profiles and soil biogenic structures. Since we know that in the North of France communities of macroinvertebrates are severely affected by high levels of heavy metal deposition (Grelle *et al.*, 2000), we hypothesize that changes in humus form occur under direct (toxicity) and indirect (changes in litter composition) effects of heavy metals.

Litter accumulation in polluted areas has been widely reported (Coughtrey *et al.*, 1979; Bengtsson & Rundgren, 1988; Ohtonen, 1994), but little work has been done in France on the influence of heavy metal deposition on humus profiles (Balabane *et al.*, 1999). Direct observation of the soil under the microscope, also called micromorphology (Kubiëna, 1943), has been shown to be essential to the knowledge of biological processes in surface soil horizons (Bernier, 1996), in particular the biogenic structures formed by several animal groups can be identified and quantified (Topoliantz *et al.*, 2000). In the present study, we used the method devised by Bernier & Ponge (1994), which enabled us to analyse the soil matrix both qualitatively and quantitatively. It is used to measure the volume of humus components, including the root systems, by a count-point procedure (Bernier & Ponge, 1994). Micromorphology describes holorganic and hemorganic horizons and also it characterizes soil biological activity by quantifying biogenic structures (Topoliantz *et al.*, 2000). By comparing the successive layers of the humus profile, it is also possible to reconstruct the recent history of the sites, especially these on which litter accumulates (Bernier & Ponge, 1994).

Material and methods

The study sites

The Bois des Asturies in Auby (Nord, France) is near and downwind of a zinc smelter which is one of the largest in the world (producing 245 000 tons of zinc per year). The

wood today suffers from active pollution by heavy metals, mainly Zn, but Cd and Pb are present in the soil from past activity. This site was formerly used to deposit slag rich in heavy metals. Hybrid poplar (*Populus sp.*) was planted in 1974 and 1977 on the site most remote from the smelter and in 1981 and 1983 nearer the smelter, after a change in production methods when electrolysis replaced coal burning. The plantation becomes sparser nearer to the smelter, due to death of most trees, and surviving ones are stunted. A sward of plants tolerant of heavy metals such as *Viola calaminaria*, *Armeria maritima halleri*, *Arrhenaterum elatius* and *Cardaminopsis halleri* covers the ground.

Three sites were studied. Site P1, 490 m from the smelter, is characterized by a field layer with *A. elatius* and *C. halleri* as dominant species, under a closed poplar canopy. Site P2, 340 m from the smelter, has a dense cover of *V. calaminaria* under an incomplete poplar canopy. There is no poplar at site P3, nearest the smelter (235 m), and the field layer is dominated by *A. maritima halleri* and *Phragmites australis*.

The soil is a silty clay loam, but the top 10 centimetres are mainly organic matter, humified and partly mixed with mineral matter in P1, but undecayed in P2 and P3. We measured soil pH and heavy metal contents at the three sites.

Earthworm sampling

We sampled lumbricid worms near the humus profiles studied. The extraction was done in six 0.5 m^2 stainless steel rings evenly spaced around the sampling point, 1 m away. Three successive waterings were performed with a diluted formalin solution at increasing concentration (3‰, 4‰, then 5‰). The worms so expelled were rinsed in tap water and preserved in formalin solution (36%) until identification at the species level. Animals extracted from the six rings were pooled to give estimates of densities for each earthworm species per square metre.

Chemical analyses

Five soil cores were taken at each of the three sites with a 5-cm diameter sample corer to 10 cm depth. Samples were air-dried at 25°C to constant weight, then stored in plastic bags until analysed.

The pH was measured electrometrically in both a 1:5 (by volume) soil:water and soil:potassium chloride (0.1 M) suspension. Total zinc, lead and cadmium were determined after solubilization of mineral matter by hydrofluoric and perchloric acids, and after preliminary destruction of organic matter by combustion at 450°C. Lead and cadmium were measured by atomic absorption at 283.3 nm and 228.0 nm, respectively and zinc by plasma emission at 213.86 nm.

Humus micromorphology

Our sampling method is described by Bernier & Ponge (1994). Our three samples (P1, P2, P3) were randomly chosen in each site, well away from the tree trunks. A block of soil 25 cm^2 in area and 10 cm deep was cut with a sharp knife, with as little disturbance as possible, and the litter and soil surrounding it were gently excavated. The various layers within the blocks were distinguished by eye in the field. Each layer was fixed immediately in 95% ethanol. The thickness of each layer was measured and annotated according to the nomenclature of Brêthes *et al.* (1995) as modified by Ponge *et al.* (2000) for mor humus. The layers were classified into OL (entire leaves), OF (fragmented leaves with faecal pellets), OH (accumulated faecal pellets), OM (mechanically fragmented leaves without faecal pellets), A (hemorganic horizon) or S (weathered horizon). When several layers were sampled in the same horizon (on the basis of visible differences), samples were numbered successively, for example OL1, OL2 and OL3. Samples of the plants

growing nearby were taken and frozen at the laboratory to help the subsequent identification of plant debris.

In the laboratory, we spread each sub-sample (layer) gently with our fingers in a petri dish, taking care not to break the aggregates; the petri dish was then filled with 95% ethanol. Plant samples from the site were also placed in alcohol. The soil specimens were examined under a dissecting microscope at x50 magnification with a cross reticule in the eye piece. A transparent film with a 200-pt grid was placed above the preparations. At each grid point, using the reticule as an aid for fixing the position, we identified and counted the material beneath it. The relative volume percentage of a given component was estimated by the ratio of the number of points identified to the total number of points inspected.

The various kinds of plant debris were identified visually by comparison with reference plant samples. Litter components (leaves, twigs) were classified according to plant species and decomposition stages on the basis of morphological features. Dead and living roots were separated by colour and turgescence state, helped when possible by observation of root sections. Animal faeces were classified according to (a) animal groups (when possible), (b) the degree of mixing of mineral matter with organic matter, and (c) colour.

Additional transect

To ensure that the three sites chosen for describing humus profiles are truly representative, we inspected soil surface horizons and took single samples for heavy metal analysis from 15 points along a transect 130-500 m from the smelter. This transect is considered representative of the range of environmental conditions on the site. At each

point we dug to 20 cm depth over a 30 cm distance and noted the thickness of surface horizons to the nearest 0.5 cm. Horizons were classified as described above.

Statistical treatment

We used Mann–Whitney non-parametric tests to compare the three sites (pH, heavy metal contents). Comparisons were done by couples, assessing whether two samples came from the same statistical population. We calculated a Bravais–Pearson correlation coefficient between the Zn content and the thickness of the OM horizon along the additional transect, where sampling was not replicated.

Results

Chemical analyses (Table 1)

The pH (in water) of the top 10 cm of the soil is similar at the three sites (6.7, 6.9 and 6.9, respectively at P1, P2 and P3). In KCl, the pHs were 6.0, 6.5 and 6.4, respectively, with a significant difference between P1 and P3.

The total zinc content of the top 10 cm of the soil increases significantly from P1 (4170 $mg.kg^{-1}$) to P2 (23 300 $mg.kg^{-1}$), then to P3 (34 800 $mg.kg^{-1}$). The lead content (839 $mg.kg^{-1}$ in P1), increases significantly in P2 and P3 (4290 and 5840 $mg.kg^{-1}$, respectively). The cadmium content at sites P2 and P3 (202 and 192 $mg.kg^{-1}$, respectively) is significantly more than at site P1 (47 $mg.kg^{-1}$). Thus site P2 is less contaminated by Zn than P3, but has similar concentrations of Pb and Cd.

Earthworm sampling

Earthworms are present at P1 (Table 1), with 103 individuals per square metre. Four species were found in this site, the most abundant ones being the epigeic *Lumbricus castaneus* (48 m^{-2}) and *Dendrodrilus rubidus* (45 m^{-2}), the least abundant one being the epigeic *Lumbricus rubellus* (8 m^{-2}) and the anecic *Aporrectodea limicola* (1.3 m^{-2}). Only four earthworms were found in the six samples collected in P2, which corresponds to a density of only 3 worms per square metre. These individuals belong to *D. rubidus* (3) and *L. rubellus* (1). There were no earthworms in site P3.

Micromorphological analyses

One hundred and five different kinds of material (Table 2) were found in the 26 layers we examined. Most are animal faeces and plant organs at varying stages of decomposition. While preparing humus blocks of soil from site P1 we found an abundant population of the millipede *Polydesmus angustus*, living in the hemorganic A horizon.

Seven layers were sampled at site P1, two in the OL horizon (0-1.5 cm) made of intact poplar and false oat litter, one in the OF horizon (1.5-3 cm) made of fragmented litter and four in the A horizon (3-10 cm), made of earthworm and millipede hemorganic faeces (Figure 1). A gradual increase in the proportion of old (broken) animal faeces was observed down the A horizon. Living mycorrhizal fine roots of poplar were most abundant in the upper part of this horizon, where fresh earthworm and millipede faeces dominated the soil matrix. Despite their large content of organic matter, shown by their black colour, hemorganic animal faeces contain numerous mineral particles, visible under the microscope. Apart from quartz, feldspar and calcite particles of silt size, we noted white globules (empty spheres) and fine shiny rust-coloured particles of silt size. Animal faeces containing rust-coloured particles are rare, and we found them only in the upper 3 cm of the A horizon. Entire poplar leaves are of normal size in OL and OF horizons, but those buried in the A horizon are stunted.

Nine layers were sampled at site P2, one in the OL horizon (0-2 cm) made of *V. calaminaria* litter, seven in the OM horizon (2-9 cm), made of matted litter and roots, and one in the upper part of the S horizon (9-10 cm) (Figure 2). Because of the accumulation of poorly transformed litter in the OM horizon, the changes in the vegetation cover can be traced over recent decades. Siliquae of *A. halleri* were present from 2 to 3 cm depth, testifying the presence of this plant species before *V. calaminaria* developed. Moss was present from 2 to 4 cm depth, showing that it covered the ground before the appearance of *A. halleri*. Below 4 cm depth, poplar litter, which was poorly represented in the top 4 cm, increased in volume while the proportion of other vegetation decreased. The transition of the OM horizon with the underlaying S horizon is sharp. The top centimetre of the S horizon is composed mainly of silt and clay, but plant tissues are present in a loose form or incorporated in the mineral matrix. Animal faeces are almost absent throughout the whole sample. Poplar roots are completely absent despite the presence of poplar litter throughout the profile. The proportion of stunted poplar leaves increases steadily from 0% in the OL horizon to 90% at 5 cm depth (Figure 3).

Ten layers were sampled at site P3, one in the OL horizon (0-1 cm), made of litter of *A. maritima halleri*, and nine in the OM horizon (1-10 cm), made of matted litter of the same species, a few roots, and pockets of mineral material increasing in volume in the lowest third of this horizon (Figure 4). Little moss is present in the OL horizon and none below. Fragmented leaves of *A. halleri* increase in volume from 0 to 6 cm then decrease until litter of *P. australis* appear (7 cm depth), together with mineral material. This material is made of amorphous masses of non faecal origin, which vary in colour from layer to layer. For example black-grey material (classes 4, 6, 37) dominates the OM7 and OM9 layers, while the OM8 layer is dominated by grey-yellow material (classes 3, 5, 36). There were no poplar remains of any sort in this profile.

Additional transect

Changes in humus forms were observed along the studied transect, running from 130 m (T15) to 500 m (T1) from the smelter (Figure 5). Mull and mor are both present. There is an abrupt passage from mull to mor at about 250 m from the smelter, between T10 and T11 (Figure 5). The sample at T10 exhibits intermediate features, with a weak (1 cm) OM horizon overlying a typical A horizon. The Zn content of the top 10 cm increases along the transect towards the smelter, from around 5000 $mg.kg^{-1}$ at 500 m distance where the humus form is mull to 20 000 $mg.kg^{-1}$ or more at 130-240 m distance where the humus form is mor. There is a sharp increase in Zn content between T10 and T11, where the humus form changes. At T12 the Zn content falls abruptly to only 5000 $mg.kg^{-1}$. This is accompanied by the appearance of an A horizon and thinning of the OM horizon (Figure 5). There is a significant linear correlation between the thickness of the OM horizon and the Zn content of topsoil horizons ($r = 0.87$).

Discussion and conclusions

Our site is heavily polluted by heavy metals, when we compare our data (Table 1, Figure 5) with the norms suggested for agricultural soils by the European Council (300 $mg.kg^{-1}$ for Zn and Pb, 3 $mg.kg^{-1}$ for Cd). Even the least polluted soil, 500 m from the smelter, is far above these thresholds. Schvartz *et al.* (1999) estimate regional background values to be 50, 15 and 0.1 $mg.kg^{-1}$ for Zn, Pb and Cd, respectively.

There was an abrupt passage from mull to mor at a threshold of about 20 000 $mg.kg^{-1}$ for Zn (Figure 5). The sharpness of the changes in humus form and in Zn content of the topsoil can be explained by a positive feed-back involving both plants and animals (Ponge *et al.*, 1999). Near the smelter plants that hyperaccumulate Zn and Cd such as *C. halleri* and *V. calaminaria* (Brooks, 1998) are abundant, especially in the sunny zone

where the planted poplar never grew properly or died (sites P2 and P3). Heavy metals concentrate in the accumulating litter of these plants, increasing the heavy metal contents of the topsoil in excess of those arising from atmospheric deposition alone (Balabane *et al.*, 1999). This is confirmed by the fact that springtail species collected from OM horizons at P2 and P3, which normally feed on fungi and decaying roots (Ponge, 2000), were found to eat mineral matter from the underlying S horizon. In contrast, farther from the smelter (site P1), mixing of organic matter with mineral matter by the anecic earthworm *A. limicola* and the millipede *P. angustus* contributed to the dilution of heavy metals, decreasing their content in the topsoil (Sterckeman *et al.*, 2000).

Can we discard possible effects of heterogeneous site conditions on humus forms, not explained by the heavy metal content of the topsoil? We have little information about the past land use before smeltering began at the turn of the nineteenth century. Most probably the site had been used for agriculture, as shown by the fertility of the loessic soil. The site is level, and the soil is a homogeneous deep loess so we believe that any effects other than those of heavy metals can be disregarded. In addition, examination of Figure 5 reveals that the sudden decrease in Zn content observed at T12 (within the zone near the smelter where the Zn content is large) coincides with the appearance of a mull A horizon, below the mor OM horizon. This shows that changes in the heavy metal content of the topsoil are matched by a change in the humus form, indicating that the humus form (and associated soil animal and microbial communities) is controlled by heavy metals.

At P2 and P3 humus profiles are of the mor type. Here there is little evidence of animal activity in the soil such as the accumulation of faecal material within A (hemorganic) or OH (holorganic) horizons. Several reasons, together, may explain the development of mor despite a nutrient-rich and easily weathered loessic parent material (Sterckeman *et al.*, 2000). Toxic heavy metals exert a selective pressure on soil organisms, reducing the diversity of functional groups when a resilience threshold is

reached (Belotti & Babel, 1993). Some animal species can adapt, becoming more resistant to heavy metals (Spurgeon & Hopkin, 2000), but there are limits to this process. Animal communities become poorer in species as pollution increases (Hågvar & Abrahamsen, 1990), and decomposition processes are severely affected by the decline of the saprophagous fauna (Hopkin, 1994). Another reason for the collapse of animal activity is that plant debris and fungal hyphae rich in heavy metals are present in the litter and are not processed by litter-feeding animals because of their resistance to microbial attack (Balabane *et al.*, 1999) or of avoidance behaviour (Filser & Hölscher, 1997). We found that sites P2 and P3 are rich in Collembola but most of the individuals feed either on aerial deposits (pollen, spores) or on the underlying substrate (silt and clay particles, with their attached microflora), thus showing the unattractive nature of the contaminated litter.

As we found earlier (Bernier & Ponge 1994), the micromorphological method used to describe humus profiles enabled us to study the recent history of sites P2 and P3. This is possible when plant debris decays slowly and does not become incorporated rapidly into the mineral soil.

At site P3 we observed a pale clayey layer at the base of the humus profile, sandwiched between two dark mineral layers. The ‘sandwich’ was created during landscaping of a spoil heap after coal was replaced by electricity as a source of energy in 1975. Poplar was planted in 1983. Just above this clayey horizon we find *P. australis* remains from the first spontaneous vegetation (Figure 4). This indicates that the soil was wet at that time, as a result of compaction of the underlying substrate. Later *P. australis* was replaced by *A. maritima halleri*, which accumulated its own litter (roots included) over the top 7 cm of the humus profile (Figure 4). This small species is very tolerant of zinc (while not accumulating the metal in its aerial parts) and is often found growing on calamine contaminated sites (Brooks, 1998). This change in the composition of the ground flora can be explained by the growth of poplar trees, which take up a lot of water

and thus decreased the moisture content of the soil. Subsequently some of the poplar trees died while some others grew poorly, probably because of the concentration of heavy metals in the soil. Mosses and lichens appear only in the top 3 cm but increase in volume in the topmost centimetre. This may indicate a recent decline in the *Armeria* population.

At site P2, where some poplar litter still falls on the ground (Figure 2), the amount of fragmented poplar leaves increases with depth. This indicates that the input of poplar litter decreased with time, as the canopy cover opened. The presence of a moss layer indicates a semi-open stage, before sun-loving plants dominated the ground layer. Stunted leaves, which dominate the leaf population of poplar in the lower half of the profile (Figure 3), may indicate a cryptogamic attack during the years following planting (Bary-Lenger *et al.*, 1992). A similar proportion of stunted leaves was found in the A horizon at P1. The hyperaccumulator *V. calaminaria* has been present on the site for a long time, since remains of its leaves and stems can be found throughout the profile (Figure 4). Nevertheless, the development of this species as a continuous carpet is probably recent, because there are no remains of other herb species in the top 2 cm though they are present below. Moss remains occur at 2-5 cm depth, accompanying a decline in poplar litter, which probably impeded the development of moss vegetation. A small amount of animal faeces occurs at 6–7 cm depth, where poplar litter is more abundant. We lack stratified heavy metal analyses but we can presume that the heavy metal content of organic topsoil horizons increased as hyperaccumulator plants progressively colonized the site, eventually suppressing saprophagous activity after a period of weak activity when poplar litter was still falling to the ground. There is no moss on the present ground surface because it has been shaded out by *V. calaminaria* which thrives on the site and is unlikely to be replaced by other vegetation under present conditions.

The soil least polluted by zinc, lead and cadmium (P1) is characterized by mull humus, with strong earthworm and millipede activity throughout the A horizon (Figure 1).

Poplar litter degrades rapidly. The large carbon content of the A horizon (estimated from the dark colour of hemorganic aggregates) might have two distinct causes. Though there is much less heavy metal contamination at P1 than at P2 and P3, the amounts are still large (Table 1). These polyvalent cations play a similar role to calcium in the stabilization of organic matter (Dupuy & Douay, 2001) and thus they too may blacken the soil (Gobat *et al.*, 1998). Another hypothesis is that this profile progressed from a dysmoder (with a thick dark OH horizon made of humified organic matter) to a mull, following a decrease in the atmospheric deposition of heavy metals. We note that in 1987 a new less-polluting process was used for zinc production. Despite intense mixing of soil horizons, the presence of shiny rust-coloured particles in the top 3 cm of the soil reflects the changes in the process at the smelter. Jarosite, a potassium iron sulphate hydroxide, was replaced by goethite (an iron oxyhydroxide). The goethite was probably transformed into haematite during the heating process, before being emitted as dust to the atmosphere. If our second hypothesis is true then we must ask where millipedes and anecic earthworms come from. Perhaps they come from nearby gardens, manure or compost heaps, or from the expansion of small relict populations at the site.

In a conclusion, we show that the micromorphological method of Bernier & Ponge (1994) enabled us to describe humus profiles of polluted soils in a way that gives a particular insight on biological trends. The plant succession, as well as the change of plant remains to humus, can be followed by comparing the various layers belonging to a profile. Pollution by heavy metals (here mainly zinc) causes changes in both vegetation and soil foodwebs, after a given threshold is reached. This threshold (here estimated to 20 000 $mg.kg^{-1}$ Zn in the topsoil) measures the resilience of the ecosystem exposed to an environmental stress originating from heavy metal toxicity. Where this threshold is exceeded, poor, unproductive vegetation replaces trees, saprophagous activity declines strongly in the topsoil, and this is reflected in a change from mull to mor.

Acknowledgements

We thank the Centre National de la Recherche Scientifique (Programme Environnement, Vie et Sociétés) for financial support within a research project directed by Professor Daniel Petit (Lille). We also thank Mr J.M. Hodgson and three anonymous referees for improving English language and clarity.

References

Balabane, M., Faivre, D., Van Oort, F. & Dahmani-Muller, H. 1999. Mutual effects of soil organic matter dynamics and heavy metals fate in a metallophyte grassland. *Environmental Pollution*, **105**, 45-54.

Bary-Lenger, A., Evrard, R. & Gathy, P. 1992. *La Forêt. Écologie, Gestion, Économie, Conservation*. Éditions du Perron, Liège, Belgium.

Belotti, E. & Babel, U. 1993. Variability in space and time and redundancy as stabilizing principles of forest humus profiles. *European Journal of Soil Biology*, **29**, 17-27.

Bengtsson, G., Gunnarsson, T. & Rundgren, S. 1983. Growth changes caused by metal uptake in a population of *Onychiurus armatus* (Collembola) feeding on metal polluted fungi. *Oikos*, **40**, 216-225.

Bengtsson, G. & Rundgren, S. 1988. The Gusum case: a brass mill and the distribution of soil Collembola. *Canadian Journal of Zoology*, **66**, 1518-1526.

Bernier N. 1996. Altitudinal changes in humus form dynamics in a spruce forest at the montane level. *Plant and Soil*, **178**, 1-28.

Bernier, N. & Ponge, J.F. 1994. Humus form dynamics during the sylvogenetic cycle in a mountain spruce forest. *Soil Biology and Biochemistry*, **26**, 183-220.

Brêthes, A., Brun, J.J., Jabiol, B., Ponge, J.F. & Toutain, F. 1995. Classification of forest humus forms: a French proposal. *Annales des Sciences Forestières*, **52**, 535-546.

Brooks, R.R. 1998. *Plants that Hyperaccumulate Heavy Metals. Their Role in Phytoremediation, Microbiology, Archaeology, Mineral Exploration and Phytomining*. CAB International, Wallingford, UK.

Coughtrey, P.J., Jones, C.H., Martin, M.H. & Shales, S.W. 1979. Litter accumulation in woodlands contaminated by Pb, Zn, Cd and Cu. *Oecologia*, **39**, 51-60.

Dupuy, N. & Douay, F. 2001. Infrared and chemometrics study of the interaction between heavy metals and organic matter in soils. *Spectrochimica Acta, Part A, Molecular Spectroscopy*, **57**, 1037-1047.

Filser, J. & Hölscher, G. 1997. Experimental studies on the reactions of Collembola to copper contamination. *Pedobiologia*, **41**, 173-178.

Gobat, J.M., Aragno, M. & Matthey, W. 1998. *Le Sol Vivant. Bases de Pédologie, Biologie des Sols*. Presses Polytechniques et Universitaires Romandes, Lausanne, Switzerland.

Grelle, C., Fabre, M.C., Leprêtre, A. & Descamps, M. 2000. Myriapod and isopod communities in soils contaminated by heavy metals in northern France. *European Journal of Soil Science*, **51**, 425-433.

Hågvar, S. & Abrahamsen, G. 1990. Microarthropoda and Enchytraeidae (Oligochaeta) in naturally lead-contaminated soil: a gradient study. *Environmental Entomology*, **19**, 1263-1277.

Hopkin, S.P. 1994. Effects of metal pollutants on decomposition processes in terrestrial ecosystems with special reference to fungivorous soil arthropods. In: *Toxic Metals in Soil/Plant Systems* (ed. S.M. Ross), pp. 303-326. John Wiley and Sons, Chichester, UK.

James, B.R. & Riha, S.J. 1986. pH buffering in forest soil organic horizons: relevance to acid precipitation. *Journal of Environmental Quality*, **15**, 229-234.

Kubiëna, W. 1943. L'investigation microscopique de l'humus. *Zeitschrift für Weltforstwirtschaft*, **10**, 387-410.

Ohtonen, R. 1994. Accumulation of organic matter along a pollution gradient: application of Odum(s theory of ecosystem energetics. *Microbial Ecology*, **27**, 43-55.

Ponge, J.F. 1999. Interaction between soil fauna and their environment. In: *Going Underground. Ecological Studies in Forest Soils* (eds N. Rastin and J. Bauhus), pp. 45-76. Research Signpost, Trivandrum, India.

Ponge, J.F. 2000. Vertical distribution of Collembola (Hexapoda) and their food resources in organic horizons of beech forests. *Biology and Fertility of Soils*, **32**, 508-522.

Ponge, J.F., Charnet, F. & Allouard, J.M. 2000. Comment distinguer dysmoder et mor? L'exemple de la forêt domaniale de Perche-Trappe (Orne). *Revue Forestière Française*, **52**, 23-37.

Ponge, J.F., Patzel, N., Delhaye, L., Devigne, E., Levieux, C., Béros, P. & Wittebroodt, R. 1999. Interactions between earthworms, litter and trees in an old-growth beech forest. *Biology and Fertility of Soils*, **29**, 360-370.

Schvartz, C., Denaix, L., Douay, F., Perdrix, E., Sterckeman, T., Wroblewski, A., Charbonnier, P. & Ledésert, B. 1999. Pathways of transfer of Pb, Cd and Zn in highly contaminated soils. In: *Modelling of Transport Processes in Soils* (eds J. Feyen & K. Wiyo), pp. 377-387. Purdue University Press, West Lafayette, Indiana.

Spurgeon, D.J. & Hopkin, S.P. 2000. The development of genetically inherited resistance to zinc in laboratory-selected generations of the earthworm *Eisenia fetida*. *Environmental Pollution*, **109**, 193-201.

Sterckeman T., Douay F., Proix N., & Fourrier, H. 2000. Vertical distribution of Cd, Pb and Zn in soils near smelters in the North of France. *Environmental Pollution*, **107**, 377-389.

Topoliantz, S., Ponge, J.F. & Viaux, P. 2000. Earthworm and enchytraeid activity under different arable farming systems, as exemplified by biogenic structures. *Plant and Soil*, **225**, 39-51.

Tranvik, L. & Eijsackers, H. 1989. On the advantage of *Folsomia fimetarioides* over *Isotomiella minor* (Collembola) in a metal polluted soil. *Oecologia*, **80**, 195-200.

Figure legends

Figure 1. Vertical distribution of the main components of the soil matrix (class numbers indicated in Table 1) at least polluted site P1. Percentage of the total matrix volume as abscissae (arbitrarily mirrorred on the negative axis for clarity).

Figure 2. Vertical distribution of the main components of the soil matrix (class numbers indicated in Table 1) at the moderately polluted site P2. Percentage of the total matrix volume as abscissae (arbitrarily mirrorred on the negative axis for clarity).

Figure 3. Changes in the proportion of stunted leaves (categories 59 and 61) within the leaf population of *Populus sp.* in the successive layers of site P2.

Figure 4. Vertical distribution of the main components of the soil matrix (class numbers indicated in Table 1) at the most polluted site P3. Percentage of the total matrix volume as abscissae (arbitrarily mirrorred on the negative axis for clarity).

Figure 5. Changes in Zn content of the topsoil and thickness of OM and A horizons along the additional transect from T1 (500 m from the smelter) to T15 (130 m from the smelter). The main vegetation features are indicated on the top line.

Table 1. Some chemical and biological features of the three sites (P1, P2 and P3). Means are followed by standard errors in parentheses when observations were replicated. The letters $_{a, b}$ indicate significant differences between sites

	P1 (490 m)	P2 (340 m)	P3 (235 m)
pH (water)	6.7 (0.2)	6.9 (0.0)	6.9 (0.1)
pH (KCl)	6.0_b (0.3)	6.4_{ab} (0.1)	6.5_a (0.1)
Zn ($mg.kg^{-1}$)	4170_c (980)	23300_b (1780)	34800_a (3860)
Pb (mg.kg-1)	839_b (165)	4290_a (226)	5840_a (1030)
Cd (mg.kg-1)	46.5_b (14.4)	202.2_a (16.6)	192.4_a (23.7)
No of earthworms/m^2	102.7	3	0

Table 2. List of the 105 classes of humus components identified in our study

N°	Class	N°	Class
1	Silt mass	**53**	Moss leaf
2	Silt mass mixed with plants fragments	**54**	Brown fragmented leaf of *Phragmites australis*
3	Yellow-grey mineral mass	**55**	Normal leaf of *Populus sp.* with nerves and little
4	Grey-black mineral mass	**56**	Brown entire normal leaf of *Populus sp.*
5	Yellow-grey hemorganic mass	**57**	Brown fragmented normal leaf of *Populus sp.*
6	Grey-black hemorganic mass	**58**	Brown fragmented leaf of *Populus sp.* + mycelium
7	Unidentified animal	**59**	Fragmented stunted leaf of Populus sp.
8	Poplar bud	**60**	Brown crumbling stunted leaf of Populus sp.
9	Brown entire poplar twig	**61**	Skeletonized stunted leaf of Populus sp.
10	Brown fragmented poplar twig	**62**	Brown crumbling normal leaf of *Populus sp.*
11	Intact poplar twig	**63**	Brown skeletonized normal leaf of *Populus sp.*
12	Poplar capsule	**64**	Light brown withered leaf of *Viola calaminaria*
13	Violet capsule	**65**	Intact leaf of *Viola calaminaria*
14	Snail shell	**66**	Fragmented grass leaf
15	Insect cuticle	**67**	Undertermined and fragmented brown leaf
16	Light brown unidentified cylindrical faeces	**68**	Flower of *Armeria maritima*
17	Dark brown unidentified cylindrical faeces	**69**	Fruit of *Armeria maritima*
18	Light brown holorganic mollusc faeces	**70**	Grass fruit
19	Brown millipede faeces with few mineral particles	**71**	Seed of *Viola calaminaria*
20	Brown holorganic millipede faeces	**72**	Lichen
21	Black hemorganic millipede faeces	**73**	Dead mycorrhizal root of *Populus sp.*
22	Black holorganic millipede faeces	**74**	Living mycorrhizal root of *Populus sp.*
23	Brown macrofauna faeces with few mineral particles	**75**	Nerve of *Phragmites australis*
24	Brown holorganic macrofauna faeces	**76**	Nerve of *Populus sp.* without lamina
25	Black altered holorganic milliped/earthworm faeces with white globules	**77**	Unidentified moss organ
26	Black altered hemorganic milliped/earthworm faeces with white globules	**78**	Brown entire petiole of *Populus sp.*
27	Black altered hemorganic milliped/earthworm faeces with fine shiny particles	**79**	Root of *Arrhenaterum elatius*
28	Brown earthworm faeces with few mineral particles	**80**	Lignified dead root of *Phragmites australis*
29	Brown holorganic earthworm faeces	**81**	Lignified living root of *Phragmites australis*
30	Black holorganic earthworm faeces with white	**82**	Lignified root of *Populus sp.*
31	Black hemorganic earthworm faeces with white	**83**	Unidentified root coated with clay particles
32	Black hemorganic earthworm faeces	**84**	Dead root of herbaceous species
33	Black hemorganic earthworm faeces with fine shiny particles	**85**	Lignified dead root of herbaceous species
34	Twig bark of *Populus sp.*	**86**	Living root of herbaceous species
35	Scale of *Populus sp.*	**87**	Lignified living root of herbaceous species
36	Yellow-grey silt particles	**88**	Moss rhizoid
37	Grey-black silt particles	**89**	Brown fragmented rhizome of *Phragmites australis*
38	Yellow silt particles	**90**	Siliqua of Arabidopsis halleri
39	Plant fragment coated with yellow-grey silt particles	**91**	Stem of *Armeria maritima*
40	Plant fragment coated with grey-black silt particles	**92**	Fragmented stem of *Arrhenaterum elatius*
41	Plant fragment coated with yellow clay particles	**93**	Brown fragmented stem of *Arrhenaterum elatius*
42	Unidentified plant fragment	**94**	Intact stem of *Arrhenaterum elatius*
43	Leaf of *Arabidopsis halleri*	**95**	Brown stem of *Arrhenaterum elatius*
44	Brown entire leaf of *Armeria maritima*	**96**	Grass stem
45	Brown fragmented leaf of *Armeria maritima*	**97**	Fragmented grass stem
46	Intact leaf of *Armeria maritima*	**98**	Moss stem
47	Leaf of *Armeria maritima* or stem of *Viola calaminaria* or *Arabidopsis halleri*	**99**	Yellow fragmented stem or rhizome of *Phragmites australis*
48	Fragmented leaf of *Arrhenaterum elatius*	**100**	Light brown withered stem of *Viola calaminaria*
49	Fragmented leaf of *Arrhenaterum elatius* +	**101**	Black withered stem of *Viola calaminaria*
50	Brown fragmented leaf of *Arrhenaterum elatius*	**102**	Brown fragmented stem of *Viola calaminaria*
51	Intact leaf of *Arrhenaterum elatius*	**103**	Intact stem of *Viola calaminaria*
52	Unidentified grass leaf	**104**	Unidentified stem
		105	Unidentified fragmented stem

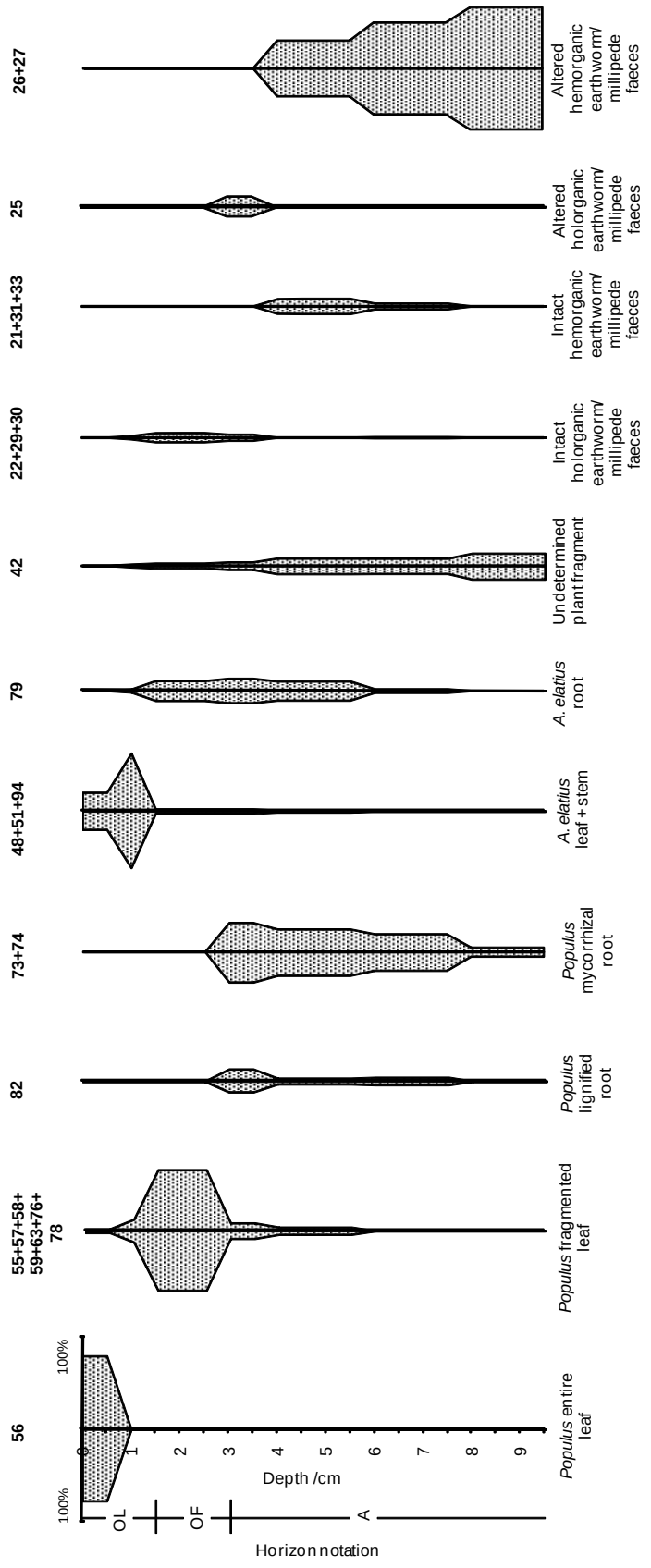
56
55+57+58+ 59+63+76+ 78
82
73+74
48+51+94
79
42
22+29+30
21+31+33
25
26+27
Populus entire leaf
Populus fragmented leaf
Populus lignified root
Populus mycorrhizal root
A. elatius leaf + stem
A. elatius root
Undetermined plant fragment
Intact holorganic earthworm/ millipede faeces
Intact hemorganic earthworm/ millipede faeces
Altered holorganic earthworm/ millipede faeces
Altered hemorganic earthworm/ millipede faeces
100%
100%
0
1
2
3
4
5
6
7
8
9
Depth /cm
OL
OF
A
Horizon notation

Fig. 1

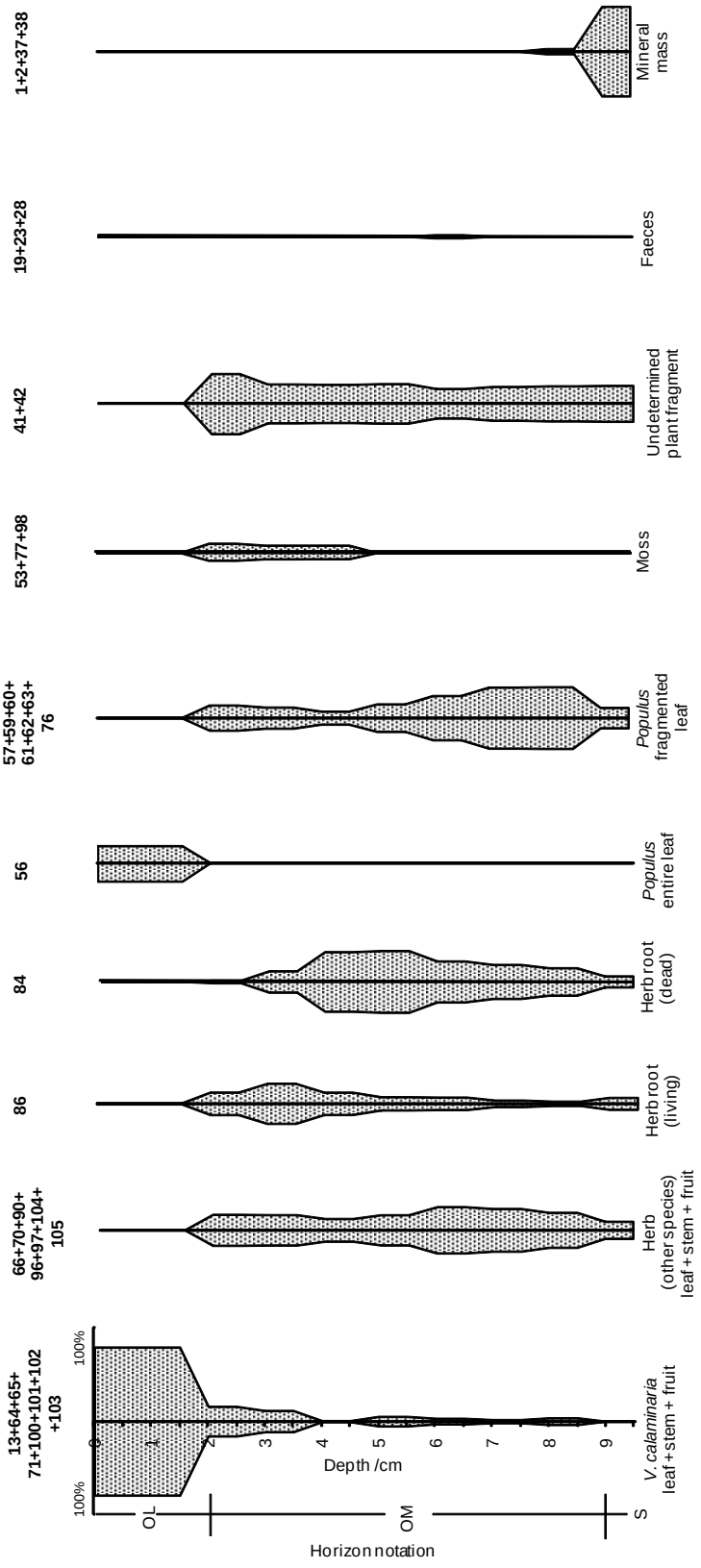
13+64+65+
71+100+101+102
+103
66+70+90+
96+97+104+
105
86
84
56
57+59+60+
61+62+63+
76
53+77+98
41+42
19+23+28
1+2+37+38
V. caespitosa
leaf + stem + fruit
Herb
(other species)
leaf + stem + fruit
Herb root
(living)
Herb root
(dead)
Populus
entire leaf
Populus
fragmented
leaf
Moss
Undetermined
plant fragment
Faeces
Mineral
mass
100%
100%
0
1
2
3
4
5
6
7
8
9
Depth /cm
OL
OM
S
Horizon notation

Fig. 2

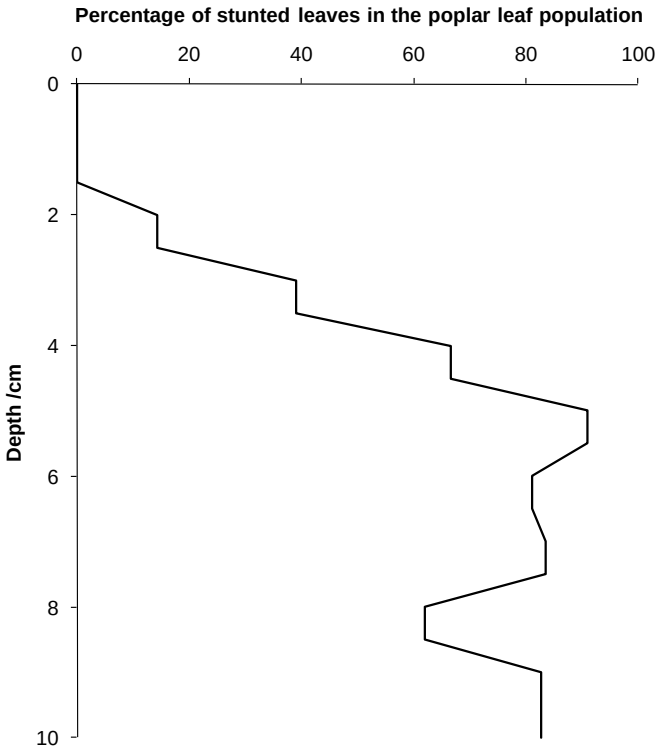
Percentage of stunted leaves in the poplar leaf population
0
20
40
60
80
100
Depth /cm
0
2
4
6
8
10

Fig. 3

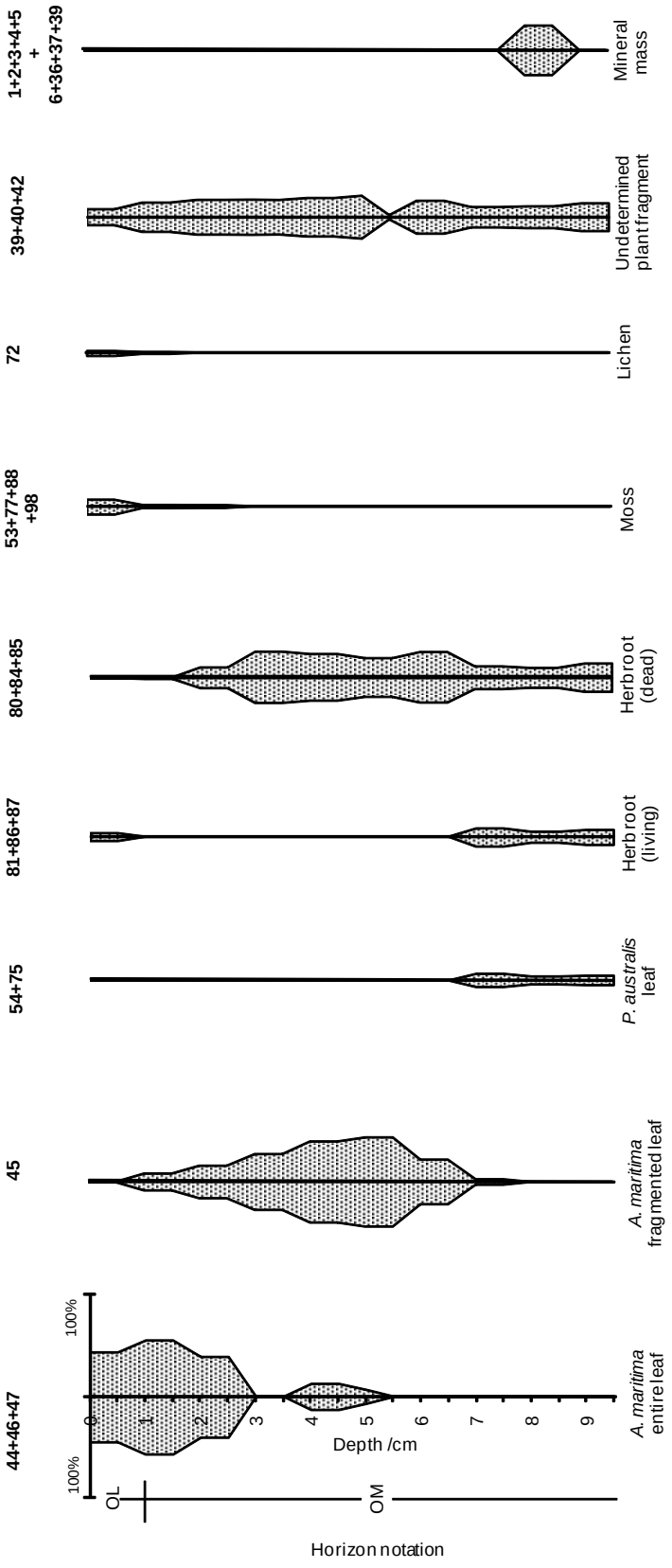
1+2+3+4+5 + 6+36+37+39
Mineral mass
39+40+42
Undetermined plant fragment
72
Lichen
53+77+88 +98
Moss
80+84+85
Herb root (dead)
81+86+87
Herb root (living)
54+75
P. australis leaf
45
A. maritima fragmented leaf
44+46+47
A. maritima entire leaf
100%
100%
0
1
2
3
4
5
6
7
8
9
Depth /cm
OL
OM
Horizon notation

Fig. 4

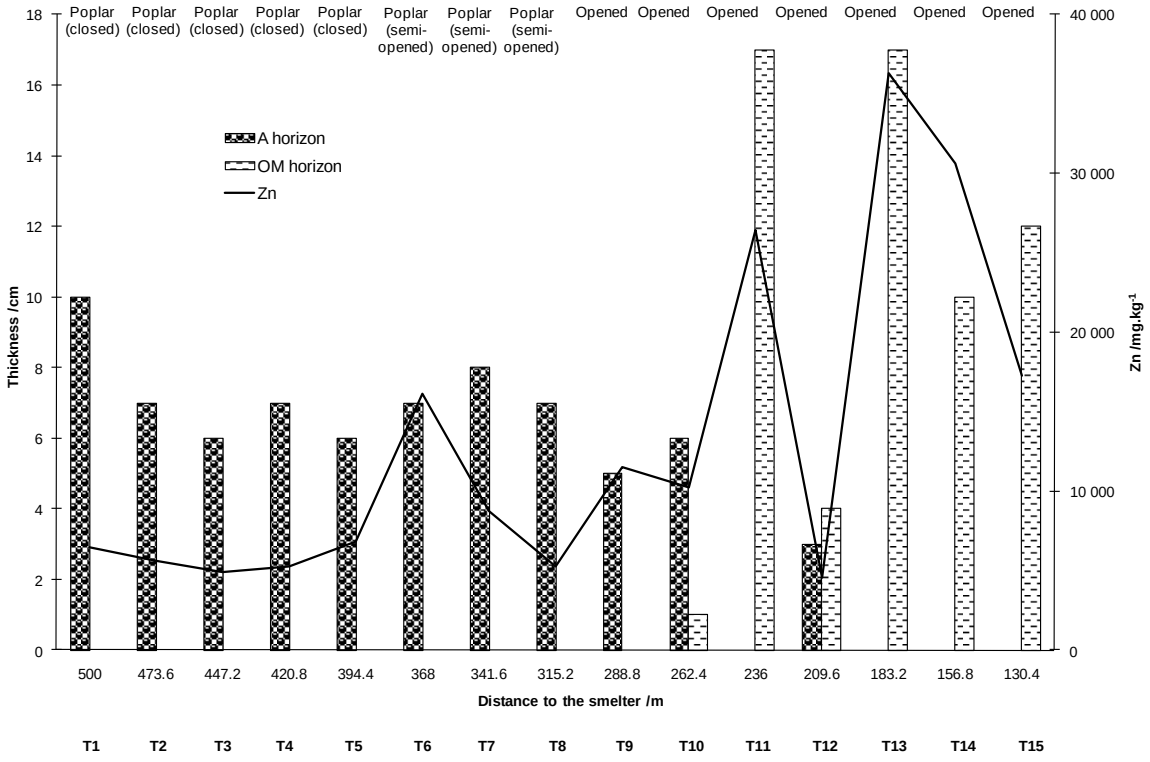
Poplar (closed)
Poplar (closed)
Poplar (closed)
Poplar (closed)
Poplar (closed)
Poplar (semi-opened)
Poplar (semi-opened)
Poplar (semi-opened)
Opened
Opened
Opened
Opened
Opened
Opened
Opened
A horizon
OM horizon
Zn
Thickness /cm
Zn /mg.kg-1
0
2
4
6
8
10
12
14
16
18
0
10 000
20 000
30 000
40 000
500
473.6
447.2
420.8
394.4
368
341.6
315.2
288.8
262.4
236
209.6
183.2
156.8
130.4
Distance to the smelter /m
T1
T2
T3
T4
T5
T6
T7
T8
T9
T10
T11
T12
T13
T14
T15

Fig. 5